ChemComm

COMMUNICATION

View Article Online
View Journal | View Issue

DNA gated photochromism and fluorescent switch in a thiazole orange modified diarylethene†

Cite this: *Chem. Commun.*, 2014, **50**, 9141

Received 15th April 2014,
Accepted 23rd June 2014

DOI: 10.1039/c4cc02783c

www.rsc.org/chemcomm

Keyin Liu,[a] Ying Wen,[a] Ting Shi,[b] Yi Li,[a] Fuyou Li,[a] Yi-lei Zhao,[b] Chunhui Huang[a] and Tao Yi*[a]

Thiazole orange-modified diarylethene (1) shows weak fluorescence but no photochromism in aqueous solution. When binding with DNA, the fluorescence of 1 is enhanced drastically and the photochromic reactivity is unlocked. This kind of DNA-responsive photoswitchable system can be used for imaging nucleic acids within cells.

The interactions of DNA and small molecules have received much attention in recent years owing to their intimate relationship with many cellular events and diseases.[1] Photoswitchable molecules can undergo conformational change between two isomers with different photophysical properties triggered by light,[2] which might have significant potential applications in DNA-related bio-events.[3] The DNA binding process or binding manner can then be adjusted by light irradiation.[4] Recently, there has been increasing interest in photochromic diarylethene derivatives owing to their high fatigue resistance, thermal irreversibility and fluorescent switchable character;[5] however, only two examples of interaction between diarylethene and DNA have been reported but without the fluorescent character. Feringa *et al.* showed that both the open and closed forms of diarylethene derivatives expressed similar binding affinity with DNA.[6] Andréasson found that enantioselectivity of the binding diarylethene species could be generated by the chiral environment of DNA in the photocyclization process.[7] However, a DNA gated photoswitchable fluorescent system may be a powerful tool to elucidate the DNA dynamics in living cells, which was rarely reported.

In a typical diarylethene analogue, the structure of diarylethene has both parallel and antiparallel conformations in equal proportions but only the antiparallel conformation can perform photoisomerization. The relative composition of parallel and antiparallel conformations, which may be controlled by an intramolecular hydrogen bond, electronic oxidation or reduction, solvent conditions, *etc.*,[8–11] can be used as a trigger to tune the gated photochromic properties of diarylethene derivatives. A biomolecule-gated photochromism might enlarge the applications of diarylethene derivatives to adjust a physiological process *in vivo*, including cell division and proliferation, intracellular physical movement, disease diagnosis and therapy. We have reported diarylethenes as photoswitchable probes for imaging living cells.[12] However, appropriate modification of diarylethene is essential to equip it with DNA-gated properties and enhance its recognition capability towards DNA.

Thiazole orange (TO) is one of the cyanine dyes[13] for DNA detection that prefers to self-aggregate in aqueous solution, resulting in photophysical variation because of the strong hydrophobic interaction and π–π stacking among the planar chromophores.[14] This easily aggregated nature of TO might make it a suitable candidate to control the conformation of diarylethene and to lock its photochromic behaviour in aqueous solution. Herein, a TO-modified diarylethene derivative (**1**) was designed and its DNA-gated photochromic properties were explored (Scheme 1). The results show that **1** acts as an effective DNA marker, whereas DNA can light-up the chromophore and unlock the photochromic activity of the diarylethene even within cells.

1 showed a difference of photophysical behavior in organic and aqueous solutions. The absorption band of **1** in the visible range centered at 504 nm (extinction coefficient, ε_{504} = 1.15 × 10^5 L mol^{-1} cm^{-1}) in an organic solvent such as acetonitrile belonged to the TO monomer (see Fig. S1a in the ESI†).[15] This absorption band blue-shifted to 476 nm (ε_{476} = 4.8 × 10^4 L mol^{-1} cm^{-1}) in water (Fig. S1b, ESI†), which was tentatively ascribed to the π → π* transition of TO in the dimer state.[16] The shape and wavelength of this absorption did not change with the increase of concentration from 10^{-7} to 10^{-5} M (Fig. S1, ESI†), suggesting no strong intermolecular interaction in this range of concentrations. The very weak fluorescence at 540 nm in acetonitrile (Q_F < 0.01%) was enhanced and red-shifted to 620 nm (Q_F = 0.25%) in water (see Fig. S2 and Table S1 in ESI†). The enlarged Stokes shift of **1** in water indicates a twisted intramolecular charge transfer in the excited states.[10]

[a] *Department of Chemistry, and Concerted Innovation Center of Chemistry for Energy Materials, Fudan University, 220 Handan Road, Shanghai 200433, P. R. China. E-mail: yitao@fudan.edu.cn*
[b] *State Key Laboratory of Microbial Metabolism, School of Life Sciences and Biotechnology, Shanghai Jiao Tong University, Shanghai 200240, P. R. China*

† Electronic supplementary information (ESI) available: Details of experiments and additional spectra. See DOI: 10.1039/c4cc02783c

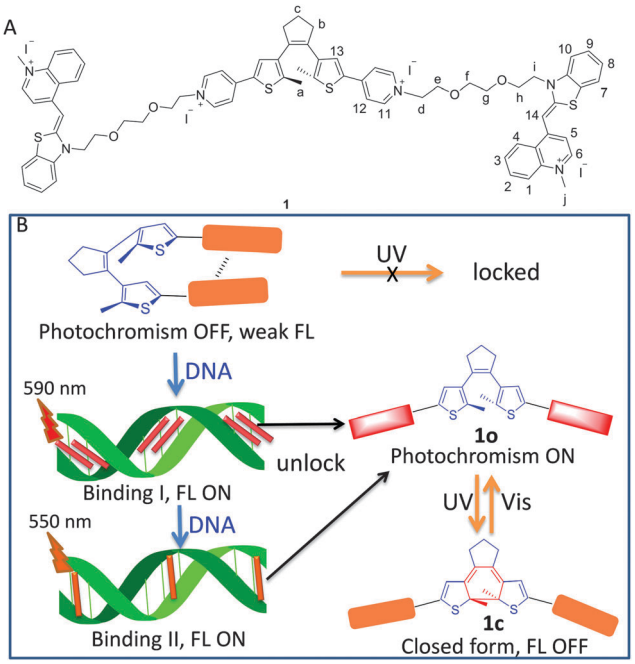

Scheme 1 (A) The structure and (B) schematic diagram of **1** responsive to DNA with gated photochromism.

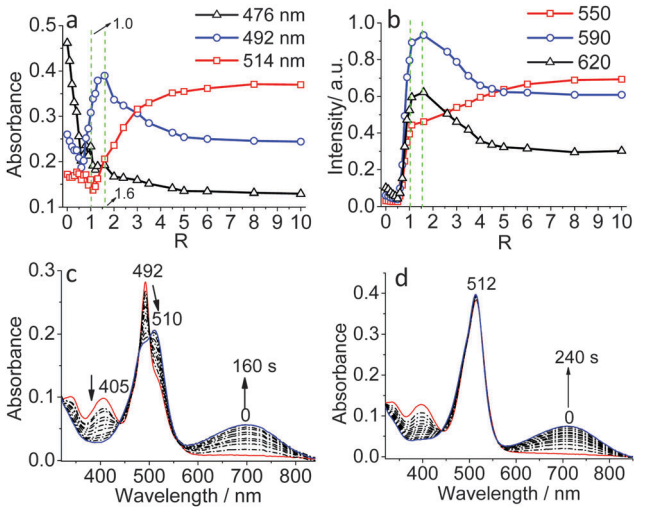

Fig. 1 (a) The absorption change at wavelengths of 476, 492 and 514 nm and (b) the fluorescence change at wavelengths of 550, 590 and 620 nm (λ_{ex} = 480 nm), respectively, with addition of AT10 to the buffer solution of **1** (5.0×10^{-6} M, 5 mM Tris-HCl, pH = 7.2), R ([bp]/[**1**]) = 1–10. The absorption change of AT10/**1** with UV light irradiation under the conditions of (c) R = 1.3 and (d) R = 10.0.

The photocyclization of **1** could occur in an organic solvent such as acetonitrile. Irradiation of red **1o** with 365 nm light led to a new absorption at 670 nm, accompanied by a decrease of absorption at 382 nm because of the enlargement of π-electron delocalization in the closed form of **1c** (Fig. S3, ESI†). The photocyclization quantum yield is 46.9%.[17] The photocyclization reaction was further proved by ^{1}H NMR spectra with the chemical shift of protons in cyclopentenyl and 2-methyl thiophene upfield-shifted from 2.12 to 1.98 ppm, 2.90 to 2.64 ppm and 7.80 to 7.32 ppm for H_a, H_b and H_{13}, respectively, upon irradiation with 365 nm light (Fig. S4, ESI†). The photocyclization transformation efficiency was 86% in the photo stationary state (PSS) as measured by the ^{1}H NMR signal. A complete reverse process can be achieved by treatment using a 670 nm wavelength laser. However, the photocyclization reaction was inactive in aqueous medium, as shown by the absorption spectral change (Fig. S5, ESI†). As the strong intramolecular interaction of TO in aqueous solution, **1** presumably exists in a folded parallel conformation (Fig. S6, ESI†). The strong correlation signals of H_a–H_{12}, H_a–H_{13}, and H_g (or H_f) with H_{11}, H_{12} and H_3, respectively, observed in the 2D NOESY spectrum in D_2O/DMSO-d_6 (96 : 4, v/v) also indicated a folded conformation of **1** in aqueous solution (Fig. S7, ESI†). Comparatively, all those Overhauser effects of **1** did not exist in CD_3CN (Fig. S8, ESI†).

The interaction of **1** with DNA was examined by absorption and emission spectra. To clearly elucidate the stoichiometric related and AT or CG base sequence determined binding patterns of **1** with DNA, two kinds of oligonucleotides with 10 base pairs (bps) per chain were used, namely poly(dA-dT)$_{10}$ (AT10), and poly(dC-dG)$_{10}$ (CG10). The absorption and emission change in different molar ratios of [bp]/[**1**] (defined as the total number of base pairs per molecule of **1**, R) reflected a multifarious configuration of **1** binding with DNA.

Upon binding with AT10, the colour change and drastic fluorescence enhancement were observed in two steps. First, with the addition of AT10 to an aqueous buffer solution of **1** in the lower R value ($R < 1.6$), an absorption band at around 492 nm increased with the decrease of the original absorption peak at 476 nm (binding I) (Fig. 1a and Fig. S9, ESI†). Correspondingly, the fluorescence was enhanced drastically and blue-shifted from 620 to 590 nm (Q_F = 2.5%) (Fig. 1b and Fig. S10a, ESI†). In the second step, upon a further increase of the bp stoichiometry ($1.6 < R < 10$), the absorption band at 492 nm decreased again and a new absorption band at 514 nm was generated with an isosbestic point at about 500 nm (binding II) (Fig. S9b, ESI†). Meanwhile, the fluorescent emission of **1** further blue shifted from 590 to 550 nm (Q_F = 3.4%), a character of the monomer state of the TO dye. The changes of the absorbance at 492 and 514 nm and the emission intensity at 590 and 620 nm, respectively, with different values of R show that binding I reaches its maximum concentration at R = 1.6, whereas the formation of binding II starts from R = 1.0 (Fig. 1a and b). All of the signals become constant when $R > 4$. The fluorescent Job's plot of **1** with addition of AT10 pbs indicates that the stoichiometry between bp and **1** in binding I and binding II modes is 1 : 1 and 3 : 1, respectively (Fig. S10b, ESI†).

Circular Dichroism (CD) spectrometry is an effective way to study the binding properties between small molecules and DNA.[18] Herein, **1** has no CD activity in aqueous solution due to lack of chirality in the open form. AT10 shows a typical diphase feature of the CD signal at the UV region.[6] A set of induced CD (ICD) signals were generated in the visible range with the addition of AT10 bps to the buffer solution of **1** in two steps. The positive ICD signals at 410, 500 and 560 nm and a

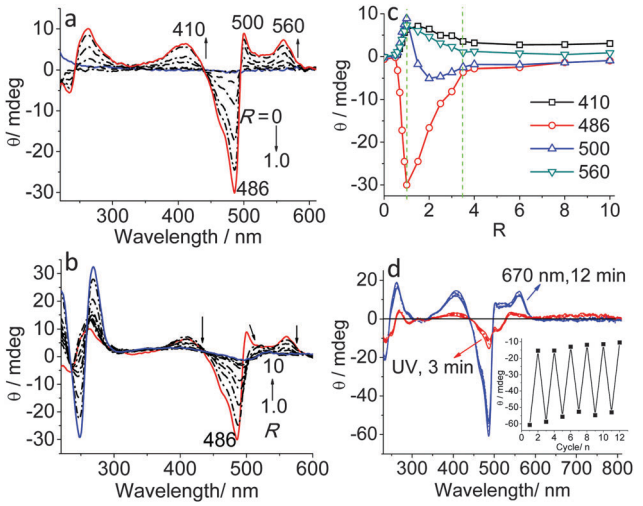

Fig. 2 (a) CD spectral change of **1** (5.0×10^{-6}) with an increasing amount of AT basepair of (a) R = 0–1.0 and (b) R = 1.0–10; (c) the CD signal changes of **1** at wavelengths of 410, 486, 500 and 560 nm with an increase of R; (d) CD spectral changes of **1**/AT10 ($C_1 = 1.4 \times 10^{-5}$, R = 2.0) with alternate irradiation of 365 and 670 nm laser light for twelve cycles; the inset shows the CD signal changes at 486 nm at the open form and PSS.

strong negative signal at 486 nm were clearly observed at $R = 0.5$ and increased to the maximum at $R = 1.0$ (Fig. 2a and c). Upon a further increase of the bp concentration ($R > 1.0$), the ICD signal at 500 nm changed to 514 nm at first and all the signals decreased to an asymptotic value when $R \geq 3.5$ (Fig. 2b and c). The above data indicate that the ICD mainly originates from the interaction of **1** and DNA in binding I mode. The strong induced positive CD for **1** in the presence of AT10 suggests that **1** binds in the minor groove to AT10 in binding I mode,[15] whereas the splitting of the ICD band into a positive and a negative component suggests the strong exciton coupling effect of the closely spaced dyes in binding I at a lower R value.[19] Because the lower R value means a lower ratio of bps but a larger ratio of molecule **1**, **1** may aggregate as a dimer in the minor groove of AT10 in binding I mode.[14] All these ICD signals obviously decreased in binding II mode, which may suggest the transformation of the binding mode from a minor groove to intercalation at a higher bp ratio ($R > 1.6$). This result is consistent with the data obtained from absorption and fluorescence spectral change.

CG10 showed a completely different binding pattern toward **1** under the same conditions. The photophysical change revealed a single binding pattern (binding II) with $R = 3$ between C·G bps and **1** (Fig. S11 and S12, ESI†). With the addition of CG10 to the buffer solution of **1** in the stoichiometry of 0–6, the absorption band at 476 nm shifted to 510 nm and the negligible fluorescence at 620 nm directly blue-shifted to 540 nm with a >100-fold increase. The binding of **1** to CG10 gives rise to a very small ICD (Fig. S13, ESI†), which supports an intercalative binding mode to GC-regions.[15] The binding interaction mode of **1** with CtDNA shows a mixed character of binding modes to AT-regions and CG-regions (Fig. S14, ESI†). However, the interaction between **1** and proteins such as bovine serum albumin showed almost no spectral change in **1** (Fig. S15, ESI†), indicating the good selectivity of **1** for bps.

It was exciting that the photochromic properties of **1** were unlocked after binding with all types of herein mentioned DNA. The reversible photoisomerization reaction could be induced by alternate irradiation with UV and visible light. A new broad absorption band centered at ~700 nm was generated and the absorption at ~400 nm decreased after irradiation with 360 nm light, accompanied by a marked decrease of fluorescence (Fig. S16–S19, ESI†). The reverse process was obtained by irradiation with visible light at 670 nm. However, the photochromic behavior of **1** differed between the two binding modes with A·T bps. In binding I, the absorption at 492 nm changed to 510 nm when treated with UV light, which could be recovered with the irradiation of 670 nm laser light (Fig. 1c and Fig. S16, ESI†). Since the absorption change at 492 and 510 nm might reflect a reversible adjustment of the two binding modes of **1** with the DNA backbone, an alternative transformation of binding I to binding II in the photochromic process was suggested. In contrast, the absorption band at 512 nm corresponding to binding II did not change in the photochromic process (Fig. 1d). Probably, the diarylethene part of **1** is much more rigid in the closed form than in the open form, which is unfavourable for a large amount of **1** to reside in the minor groove of A·T DNA due to the spatial block.

Similar to the change observed in absorption and fluorescent spectra, the photochromic process can tune the ICD of **1** binding to AT10. When UV light was used for irradiation, all of the original ICD signals decreased sharply, together with a new broad ICD band generated in the NIR region (600–800 nm) and treatment with visible light can recover the initial state (Fig. 2d and Fig. S20, ESI†). The CD signals reflected the aggregation pathways of dyes along the double helix structure of the DNA, thus, reversible adjustment of the CD spectrum in the photoisomerization process might be a hint of change among different self-assembly patterns between **1** and bps. These results indicate that DNA can act as a trigger to control the photochromism of **1** and the triggered photochromic process can reflect the binding mode of **1** with DNA. Moreover, the DNA-mediated photochromic system maintained high fatigue resistance and could be repeated tens of times with only 10% of spectral change (Fig. 2b, inset and Fig. S17c, ESI†).

Using confocal laser scanning microscopy (CLSM), the intracellular behavior of **1** was explored in a Hela cell line. Intense fluorescence was observed in the nucleolus area when **1** was incubated with fixed Hela cells, which could be co-localized with the commercial nucleus localization dye Hoechst33258 (Fig. 3a–d) and shown by a 3D z-axis scan in CLSM (Fig. S21, ESI†). The weak fluorescence of **1** was observed also in the plasma area, with a signal distribution ratio of 7.5 : 1 between nucleolus and plasma (Fig. 3e and f). The DNA-mediated photochromism can be *in situ* performed in cell medium with alternate irradiation of UV and visible laser light equipped by CLSM. When a selected cell was irradiated with a 405 nm light for 15 min, the fluorescence was gradually bleached, which indicated that the majority of **1** was transformed from the open to the closed form. When it was treated with light at a wavelength of 633 nm, complete recovery of the fluorescence was observed in 3 min (Fig. 3h and Fig. S22, ESI†). The optical switching process can be repeated many

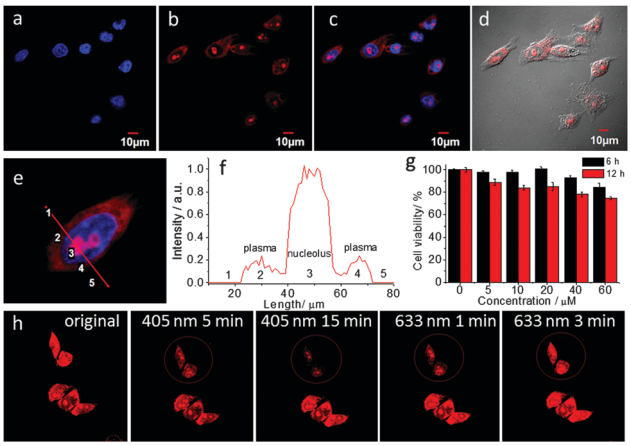

Fig. 3 (a–d) CLSM images of fixed Hela cells incubated with **1** (10 μM) for 10 min followed by Hoechst33258 (10 μM) for 30 min at 37 °C; (a) Hoechst33258 in the blue channel (420–480 nm), (b) **1** in the red channel (520–620 nm), (c) overlay of Hoechst33258 and **1** and (d) overlay image of (b) and the bright field image. (e) A selected cell and (f) cross-sectional analysis along the red line in image (e). (g) Cell viability value (%) by the MTT method. (h) Fluorescent images of selected cells in red circles bleached with 405 nm and recovered using a 633 nm laser.

times without any noticeable decrease of fluorescence. The high fatigue and photo bleaching resistance property of **1** are much superior compared to other traditional fluorophores. The cytotoxicity evaluation of **1** is essential for its further biological application, thus, the effect on cell proliferation was checked by a MTT assay (ESI†). After incubation for 12 h in the presence of 5.0–60.0 μM **1**, more than 90% cell viability was observed in concentrations below 20 μM, a low level of toxicity (Fig. 3g). Potentially, **1** can be used as a nucleolus labeling agent with photochromic properties.

In conclusion, a DNA-gated photochromism based on diarylethene thiazole orange was developed. **1** exhibited different interaction modes toward A·T and C·G base pairs with a great diversity of photophysical properties. DNA acted as a key to tune the parallel and antiparallel conformations of diarylethene species and induced fluorescence in both solution and intracellular images. This is a specific example of a biomolecular-controllable photoreaction, which might allow the application of light to a combination of biomolecules and stimuli-responsive materials to build new functional molecular devices and provide new insight into the bio-application of photochromic materials in the future.

The authors are grateful for the financial support from 973 (2013CB733700), NNSFC (21125104, 51373039), PIRTU (IRT1117) and Shanghai Sci. Tech. Comm. (12XD1405900).

Notes and references

1 H. Niyazi, J. P. Hall, K. O'Sullivan, G. Winter, T. Sorensen, J. M. Kelly and C. J. Cardin, *Nat. Chem.*, 2012, **4**, 621; J. Wu, Y. Zou, C. Li, W. Sicking, I. Piantanida, T. Yi and C. Schmuck, *J. Am. Chem. Soc.*, 2012, **134**, 1958; S. Ikeda, T. Kubota, M. Yuki and A. Okamoto, *Angew. Chem., Int. Ed.*, 2009, **48**, 6480.
2 J. J. Zhang, Q. Zou and H. Tian, *Adv. Mater.*, 2013, **25**, 378; C. Yun, J. You, J. Kim, J. Huh and E. Kim, *J. Photochem. Photobiol., C*, 2009, **10**, 111; M. Singer and A. Jäschke, *J. Am. Chem. Soc.*, 2010, **132**, 8372; Y. Shiraishi, S. Sumiya and T. Hirai, *Chem. Commun.*, 2011, **47**, 4953; M. McCullagh, I. Franco, M. A. Ratner and G. C. Schatz, *J. Am. Chem. Soc.*, 2011, **133**, 3452.
3 A. A. Beharry and G. A. Woolley, *Chem. Soc. Rev.*, 2011, **40**, 4422; J. Andersson, S. Li, P. Lincoln and J. Andréasson, *J. Am. Chem. Soc.*, 2008, **130**, 11836; D. Berdnikova, O. Fedorova, E. Gulakova and H. Ihmels, *Chem. Commun.*, 2012, **48**, 4603.
4 C. Dohno and K. Nakatani, *Chem. Soc. Rev.*, 2011, **40**, 5718.
5 M. Irie, *Photochem. Photobiol. Sci.*, 2010, **9**, 1535; M. Irie, *Chem. Rev.*, 2000, **100**, 1685; H. Tian and S. Yang, *Chem. Soc. Rev.*, 2004, **33**, 85; S. Yagai, K. Iwai, M. Yamauchi, T. Karatsu, A. Kitamura, S. Uemura, M. Morimoto, H. Wang and F. Würthner, *Angew. Chem.*, 2014, **126**, 2640.
6 A. Mammana, G. T. Carroll, J. Areephong and B. L. Feringa, *J. Phys. Chem. B*, 2011, **115**, 11581.
7 T. C. S. Pace, V. Müller, S. Li, P. Lincoln and J. Andréasson, *Angew. Chem., Int. Ed.*, 2013, **52**, 4393.
8 M. Ohsumi, T. Fukaminato and M. Irie, *Chem. Commun.*, 2005, 3921; F. Nourmohammadian, T. Q. Wu and N. R. Branda, *Chem. Commun.*, 2011, **47**, 10954; J. Massaad, J. C. Micheau, C. Coudret, R. Sanchez, G. Guirado and S. Delbaere, *Chem. – Eur. J.*, 2012, **18**, 6568.
9 X. C. Li, Y. Z. Ma, B. C. Wang and G. G. Li, *Org. Lett.*, 2008, **10**, 3639.
10 M. Irie and K. Sayo, *J. Phys. Chem.*, 1992, **96**, 7671; M. Irie, O. Miyatake and K. Uchida, *J. Am. Chem. Soc.*, 1992, **114**, 8715.
11 Y. Wu, S. Chen, Y. Yang, Q. Zhang, Y. Xie, H. Tian and W. Zhu, *Chem. Commun.*, 2012, **48**, 528; D. Dulic, T. Kudernac, A. Puzys, B. L. Feringa and B. J. van Wees, *Adv. Mater.*, 2007, **19**, 2898; Y. Ishibashi, M. Mukaida, M. Falkenstrom, H. Miyasaka, S. Kobatake and M. Irie, *Phys. Chem. Chem. Phys.*, 2009, **11**, 2640.
12 Y. Zou, T. Yi, S. Xiao, F. Li, C. Li, X. Gao, J. Wu, M. Yu and C. Huang, *J. Am. Chem. Soc.*, 2008, **130**, 15750; X. Piao, Y. Zou, J. Wu, C. Li and T. Yi, *Org. Lett.*, 2009, **11**, 3818.
13 K. C. Hannah and B. A. Armitage, *Acc. Chem. Res.*, 2004, **37**, 845; L. Yuan, W. Lin, K. Zheng, L. He and W. Huang, *Chem. Soc. Rev.*, 2013, **42**, 622.
14 T. Y. Ogul'chansky, M. Y. Losytskyy, V. B. Kovalska, V. M. Yashchuk and S. M. Yarmoluk, *Spectrochim. Acta, Part A*, 2001, **57**, 1525.
15 H. J. Karlsson, P. Lincoln and G. Westman, *Bioorg. Med. Chem.*, 2003, **11**, 1035.
16 A. Biancardi, T. Biver, A. Marini, B. Mennucci and F. Secco, *Phys. Chem. Chem. Phys.*, 2011, **13**, 12595.
17 S. Chen, Y. Yang, Y. Wu, H. Tian and W. Zhu, *J. Mater. Chem.*, 2012, **22**, 5486.
18 N. Inukai, T. Kawai and J. Yuasa, *Chem. Commun.*, 2011, **47**, 9128; D. Strat, S. Missailidis and A. F. Drake, *ChemPhysChem*, 2007, **8**, 270.
19 J. K. Choi, A. D'Urso, M. Trauernicht, M. Shabbir-Hussain, A. E. Holmes and M. Balaz, *Int. J. Mol. Sci.*, 2011, **12**, 8052.

